

Original Article

The effects of miR-151 on LPS-induced ARDS rats and its functional mechanisms

Xiangjuan Chen¹, Wanjun Huang², Xiaoyang Xu², Xuanli Zhang², Jiayang Fu², Xiao Han², Zongji Shen¹

¹Department of Obstetrics and Gynecology, The First Affiliated Hospital of Soochow University, Suzhou 215006, Jiangsu, China; ²Department of Obstetrics and Gynecology, The First Affiliated Hospital of Wenzhou Medical University, Wenzhou 325027, Zhejiang, China

Received June 4, 2018; Accepted January 11, 2019; Epub September 15, 2019; Published September 30, 2019

Abstract: Acute respiratory distress syndrome (ARDS) is a critical condition often seen in respiratory clinics. MicroRNA-151 (miR-151) plays crucial roles in respiratory disease. However, its functions and mechanisms on lipopolysaccharide (LPS) induced ARDS rats have not been reported. Wistar rats were randomly assigned into a normal control group, an ARDS group which received 5 µg/g LPS injection for model preparation, and an miR-151 group which received lentivirus transfection on ARDS rats. Real-time quantitative PCR was employed to measure miR-151 expression. The arterial blood gas index was measured, along with the wet/dry (W/D) ratio of lung tissues, myeloperoxidase (MPO) and superoxide dismutase (SOD) activity, and the protein content and cell count in bronchoalveolar lavage fluid (BALF). An ELISA assay was used to measure the expressions of tumor necrosis factor-α (TNF-α) and interleukin-2 (IL-2). Real-time PCR and Western blot were adopted to measure the pulmonary expression of NF-κB mRNA and protein. The ARDS group had decreased miR-151 expression, suppressed arterial blood-gas and SOD, plus a higher W/D ratio and MPO. The protein content and cell count of BALF were increased in the ARDS rats, which had higher TNF-α, IL-2, and NF-κB expressions ($P < 0.05$ compared to the control group). The MiR-151 group showed a remarkable improvement of the blood-gas index and had a lower W/D ratio, MPO activity, a higher SOD activity, and decreased expression of TNF-α, IL-2, and NF-κB ($P < 0.05$ compared to the ARDS group). miR-151 showed down-regulation in the rat ARDS model. miR-151 regulation can suppress NF-κB expression by modulating oxidative stress and alleviating inflammation, thus improving pathological changes in ARDS rats.

Keywords: miR-151, acute respiratory distress syndrome, oxidative stress, inflammation, NF-κB

Introduction

Acute respiratory distress syndrome (ARDS) is a critical condition often seen in respiratory clinics, and with a mortality rate as high as 50%, it has drawn interest from critical medicine clinicians [1, 2]. ARDS has multiple inducing factors and can be caused by pneumonitis, abnormal expiration, pulmonary contusion, intrapulmonary/systemic severe infection, or severe lung injury. Various lethal factors can cause diffused damage to lung tissues and lead to clinical syndromes characterized by refractory hypoxia and progressive respiratory stress [3, 4]. ARDS is also the pulmonary presentation of systemic inflammation response syndrome (SIRS) or multi-organ dysfunction [5]. ARDS has complicated pathogenic mechanisms,

and its major pathological features include inflammatory cascade injury on vascular endothelial cells, neutrophils aggregation in lung mesenchyme and alveolus, leading to increased permeability of pulmonary vessels causing pulmonary edema [6]. Among multiple inducing factors, sepsis can lead to high a incidence of ARDS with early onset [7, 8]. Due to the important factors contributing to ARDS, sepsis complicated with ARDS commonly occurs in intensive care units (ICU) and has a high mortality rate [9]. The occurrence of sepsis is closely related to the bacterial release of lipopolysaccharides (LPS) in plasma [10].

MicroRNA (miR) is widely distributed in both animal and plant cells and is a group of small molecule RNA with biological functions [11, 12].

microRNA is a group of small molecular RNA containing 19~25 nucleotides, sharing similar molecular biological features [13, 14]. MiR-151 plays crucial roles in the progression of respiratory diseases [15]. However, the expression and related mechanisms of miR-151 in ARDS are still unclear. This study thus established an LPS-induced ARDS rat model, on which the functional role and related mechanism of miR-151 on ARDS was analyzed.

Materials and methods

Experimental animals

A total of 60 healthy Wistar rats (2 months old, SPF grade, body weight 250 ± 20 g) were purchased from the laboratory animal center of Soochow University and were kept in an SPF grade facility. The temperature was fixed at $21 \pm 1^\circ\text{C}$, with the relative humidity set at 50-70%, and a 12 h light/dark cycle was maintained. All animal experiments were performed by experienced technicians following protocols that were approved by the ethical committee of The First Affiliated Hospital of Soochow University.

Reagents and equipment

Sodium pentobarbital was purchased from Beijing Chemical Reagents Company (China). The test kits for MPO and SOD were purchased from Jiancheng Bioengineering (China). The chemical reagents for Western blot were purchased from Beyotime (China). The ECL reagent was purchased from Amersham Bioscience (US). Rabbit anti-mouse NF- κ B monoclonal antibody and goat anti-rabbit horseradish peroxidase labelled IgG secondary antibody were purchased from Cell Signaling (US). The ELISA kits for TNF- α and IL-2 were purchased from R&D (US). The lentivirus vector for miR-151 was constructed by Jikai Gene (China). The RNA extraction kit and the reverse transcription kit were purchased from Axygen (US). Other common reagents were purchased from Sango Bio (China). A Model 7700 fluorescent quantitative PCR cycler was purchased from ABI (US). A Labsystem Version 1.3.1 microplate reader was purchased from Bio-Rad (US). A blood gas analyzer for small animals was purchased from Nova Biomedical (US). A UV spectrophotometer

was purchased from METTLER TOLEDO (Sweden).

Animal model preparation and grouping

A total of 60 healthy male Wistar rats, fed normally for 2 weeks, were randomly assigned into three groups (N=20 each), including a normal control group, an ARDS group, which received 5 $\mu\text{g/g}$ LPS to prepare a rat ARDS model, and an miR-151 group that received an miR-151 lentivirus transfection on ARDS model rats.

Preparation of rat ARDS model by LPS and treatment

Based on previous studies [16], the rats were anesthetized using 50 mg/kg sodium pentobarbital (1%) via intraperitoneal injection. The rats were fixed on a table, and an incision was made on the neck to expose the trachea, into which 5 $\mu\text{g/g}$ LPS was slowly dropped for even distribution into bilateral lung tissues. After suturing the incision by layers, 24 ml/kg saline was injected for fluid replenishment. The control group received a similar treatment to those in the model group, except that an equal volume of PBS was used instead of LPS. Lentivirus vector and miR plasmid were co-transfected into the 293T cell line kept in-house. Viral particles were packaged, collected and condensed. A 4×10^7 IU viral vector containing the miR-151 plasmid was infused via the trachea during the model preparation.

Sample tissue collection

6 h after treatment, all three rat groups were anesthetized using 10% hydrate chloral. Blood samples were collected from the abdominal aortae and were centrifuged at 2000 rpm for 10 min to extract the serum from the upper layer. Serum samples were separated and kept at -20°C . The rats were sacrificed, and the left upper lung lobule tissue from each was collected to measure the wet/dry (W/D) ratio. Other lung tissues were kept at -80°C .

Histochemistry analysis of lung tissue

The lung tissue was collected, fixed in formalin (10%) for 24-48 hrs and then placed in ethanol until being put in paraffin, sectioned (5 μm) and stained with hematoxylin and eosin (HE).

Table 1. Synthesized primer sequence

Gene	Forward primer 5'-3'	Reverse primer 5'-3'
GADPH	AGTGCCAGCCTCGTCTCATAG	CGTTGAACCTTGCCGTGGGTAG
miR-151	GCAGGGAATCCCAAGGGTT	GGAGTTGATGTCTTCGCGTC
NF-κB	GATATCCAGGGAGTTGGGA	ATGTCCAGGGTTCATTGGTCTGT

Blood-gas analysis and W/D assay

A blood-gas analyzer was used to quantify the arterial blood oxygen pressure (PaO₂) in all groups of rats, and the pH values were determined also. The surface water on the left upper pulmonary lobules was removed by filtered water. The wet weight of the lung tissues was measured. The lung tissues were then dried for 24 h in preparation for measuring their dry weight. The W/D ratio was calculated to evaluate the condition of the pulmonary edema.

Assay for lung tissue MPO activity

Following the test kit's instruction manual, 100 mg cryopreserved lung tissues were homogenized on a cold phosphate potassium buffer and were centrifuged at 4°C with 30000 g for 30 min. The precipitation was re-suspended in a 50 mmol/L phosphate potassium buffer. After a 60°C water-bath for 2 h, the mixture was centrifuged at 4°C with 40000 g for 130 min. The supernatant was retracted and was mixed with a reaction buffer. The absorbance value (A) was measured by UV spectrometry at a wavelength of 460 nm. MPO activity (in U/g) = A × 13.5/lung wet weight (g).

Analysis of SOD activity in rat pulmonary tissues

The activity of SOD was detected in rat pulmonary tissues following the test kit's instruction manual. In brief, the lung tissue proteins were extracted, denatured in a 95°C water-bath for 40 min, and then rinsed in cold water. After a 4000 rpm centrifugation for 10 min, an ethanol-chloroform mixture (5:3 in v/v) was used to extract the ethanol phase in tissue homogenate for measuring LDH and total SOD activity.

BALF protein quantification and cell count

Following the test kit's instruction manual, the BCA approach was used to measure the protein content of BALF. A standard curve for proteins

was plotted based on the concentration of standard curves. The A values at 565 nm were measured to deduce the sample protein content based on the standard curve and were presented as mg/ml. Increased values of protein thus

indicated an increased permeability of pulmonary micro vessels. BALF samples were centrifuged and the cell precipitation was re-suspended into 0.1 ml saline for preparing the smear slides. Under the microscope, 200 cells were counted for neutrophils and lymphocytes.

Real-time PCR

Real-time PCR was used to measure the expressions of NF-κB mRNA and miR-151. Under sterile conditions, lung tissue mRNA was extracted using Trizol reagent on ice, and cDNA was synthesized using relevant primers (**Table 1**). Real-time PCR was then used to quantify target gene expressions under the following conditions: 52°C for 1 min, followed by 35 cycles each containing 90°C 30 s, 58°C 50 s and 72°C 35 s. For RAGE and NF-κB, conditions were: 55°C for 1 min, followed by 90°C 30 s, 62°C 50 s and 72°C 35 s in 35 cycles. A fluorescent quantitative PCR cycler was used to collect data. CT values were calculated based on the internal reference gene GAPDH to plot the standard curve. The quantitative analysis was performed using the 2^{-ΔCt} approach.

ELISA assay for serum TNF-α and IL-2 expression

The serum samples collected from all the groups of rats were kept at -80°C. An ELISA kit was used to detect the expression of TNF-α and IL-2 in the supernatant. The experimental protocols followed the ELISA kit's instruction manual. Following a concentration of standard samples and relevant A values, a linear regression function was plotted, and sample concentration was calculated on the regression function based on the A values of the samples.

Western blot for NF-κB protein expression

Nuclear and cytoplasmic protein was isolated using a Nuclear and Cytoplasmic Protein Extraction kit (Beyotime Biotechnology, catalogue number: P0027, Nantong, China) according to manufacturer's instructions. For the Western

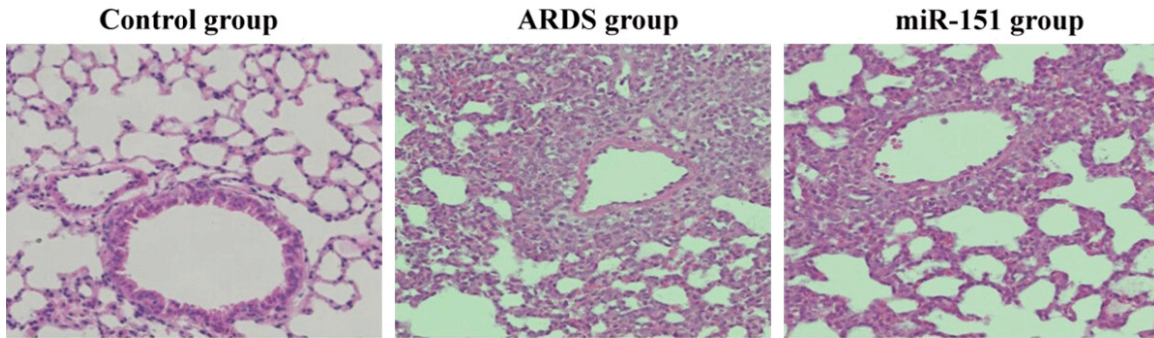


Figure 1. HE staining of lung tissue. Each lung was isolated from the mice in the different groups followed by being fixed, sectioned and stained with HE for the analysis of the pathological changes of the lung.

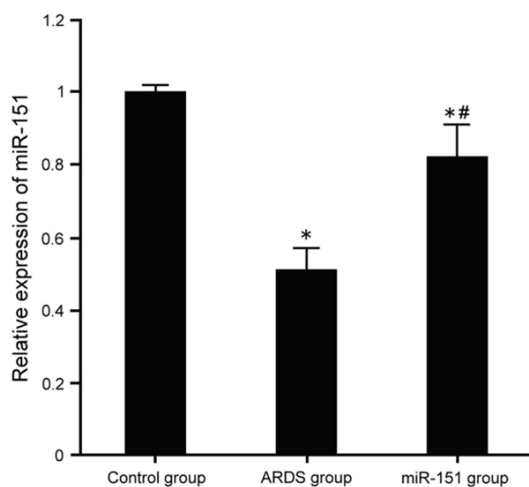


Figure 2. Expressional change of miR-151 in rat lung tissues. * $P < 0.05$ compared to the control group; # $P < 0.05$ compared to the ARDS group.

blotting assay, the proteins were separated by 10% SDS-PAGE and were transferred to a PVDF membrane under 100 mA for 1.5 h. Non-specific binding backgrounds were removed with 5% defatted milk powder incubation for 2 h at room temperature. A primary antibody against NF- κ B p65, p-p65, Histone H3.1, GAPDH (1:500 dilution) was added for a 4°C overnight incubation. On the next day, the membrane was washed in PBST and was cultured within 1:2000 diluted goat anti-rabbit secondary antibody for 30 min and then incubated at room temperature. After PBST washing, the membrane was developed for 1 min for the X-ray film exposure. Protein imaging processing and Quantity One software were used for the scanning of the X-ray film and for measuring the band density. All the experiments were per-

formed four times ($n=4$) for the statistical analysis.

Statistical processing

SPSS 16.0 software was used for the statistical analysis. Measurement data were presented as the mean \pm standard deviation (SD). The comparison of the means across multiple groups was performed using one-way analysis of variance (ANOVA). Statistical significance was defined when $P < 0.05$.

Results

Lung pathological changes

HE staining was performed to evaluate the pathological changes of the lungs in the different groups. As seen in **Figure 1**, the alveolar structure of the lung tissue in the control group was clear without inflammatory cell infiltration around the small trachea at the end of alveoli. The ARDS group showed an unclear alveolar lung tissue structure and a reduced diameter of the small trachea at the end of alveolar as well as a decreased alveolar volume due to the infiltration of a large number of inflammatory cells. However, reduced inflammatory cell infiltration and increased alveolar volume were found in the miR-151 group.

Expression change of miR-151 in rat pulmonary tissues

Real-time PCR was used to analyze the expressional change of miR-151 in rat lung tissues. The results showed that ARDS rats had a significantly decreased expression of miR-151 ($P < 0.05$ compared to the control group). A lenti-

Table 2. Comparison of blood-gas analysis and W/D

Group	PaO ₂ (mmHg)	pH	W/D
Control	125.22 ± 23.21	7.36 ± 0.06	4.21 ± 0.41
ARDS	52.21 ± 11.73*	6.51 ± 0.05*	7.89 ± 0.72*
miR-151	101.76 ± 15.21*#	6.9 ± 0.06*#	6.12 ± 0.51*#

*P<0.05 comparing to control group; #P<0.05 comparing to ARDS group.

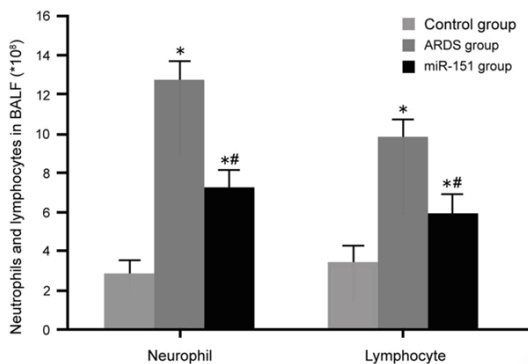


Figure 3. Cell count of BALF cells in rats. *P<0.05 compared to the control group; #P<0.05 compared to the ARDS group.

virus vector was used to transfect miR-151 into ARDS rats for up-regulation (P<0.05 comparing to ARDS group, **Figure 2**).

Blood-gas analysis and W/D ration comparison among all the groups of rats

We further tested arterial PaO₂, pH and blood-gas indexes among all the groups of rats, and we measured the W/D ratio of rat lung tissues to evaluate the severity of pulmonary edema. The results indicated that ARDS induced a significant decrease of PaO₂ and pH values (P<0.05 compared to the control group). After up-regulating miR-151, the PaO₂ and pH values of the ARDS rats were significantly elevated (P<0.05 compared to the ARDS group). The ARDS rats also had an elevated W/D ratio of lung tissues (P<0.05 comparing to control group). The up-regulation of miR-151 also decreased the W/D ratio of the lung tissues (P<0.05 compared to the ARDS group, **Table 2**).

Enumeration of BALF cells

The different types of cells in BALF were enumerated. The results showed a significant increase of neutrophils and lymphocytes in the

BALF from the ARDS group (P<0.05 compared to the control group). The up-regulation of miR-151 significantly suppressed the number of neutrophils and lymphocytes in the BALF of the ARDS rats (P<0.05 compared to the ARDS group, **Figure 3**).

Change of oxidative stress among all groups of rats

We further measured the activity change of MPO and SOD in rat pulmonary tissues from all groups. The results showed a significant increase of MPO activity plus a lower SOD content in the lung tissues after ARDS (P<0.05 compared to the control group). The up-regulation of miR-151 can remarkably inhibit MPO activity and enhance SOD content (P<0.05 compared to the ARDS group, **Table 3**).

Serum TNF-α and IL-2 expression in rats

We employed an ELISA assay to measure the serum expression of TNF-α and IL-2. The results indicated significantly elevated serum TNF-α and IL-2 in the ARDS rats (P<0.05 compared to the control group). The up-regulation of miR-151 remarkably inhibited serum TNF-α and IL-2 expressions in the ARDS rat serum (P<0.05 compared to the ARDS group, **Figure 4**).

mRNA and protein expression of NF-κB in rat lung tissues

Real-time PCR and Western blot were used to measure the effect of miR-151 on mRNA and the protein expression of NF-κB in ARDS rat lung tissues. The results showed significantly elevated NF-κB mRNA expression in ARDS rat lung tissues (P<0.05 compared to the control group) (**Figure 5A**). The up-regulation of miR-151 significantly inhibited the expression of NF-κB mRNA expression as well as nuclear p65 and cytoplasm p-p65 (**Figure 5B, 5C**) in lung tissues (P<0.05 compared to the ARDS group).

Discussion

ARDS caused diffused structural changes in pulmonary tissues, leading to an increased permeability of lung alveolar micro vessels and large amounts of protein containing edema fluid inside the lung tissues that cannot be effectively cleared [17]. The most important

Table 3. Oxidative stress index for all groups of rats

Parameters	Control group	ARDS group	miR-151 group
MPO (U/g)	2.17 ± 0.68	9.75 ± 1.21*	5.31 ± 1.17*#
SOD (U/mg)	31.22 ± 5.18	13.23 ± 4.51*	21.21 ± 6.12*#

* $P < 0.05$ compared to the control group; # $P < 0.05$ compared to the ARDS group.

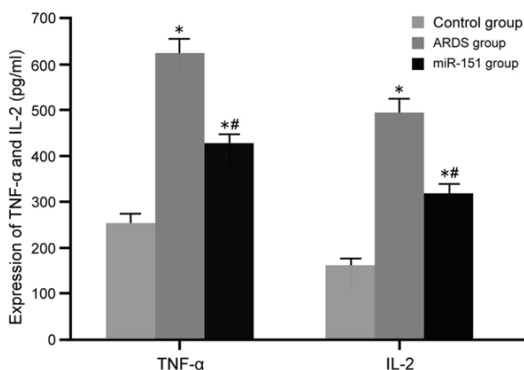


Figure 4. Expression of serum TNF- α and IL-2 expression in rats. * $P < 0.05$ compared to the control group; # $P < 0.05$ compared to the ARDS group.

pathological reason for ARDS is pulmonary inflammation and edema, leading to alveolar wall collapse and respiratory dysfunction [18]. This study utilized LPS to prepare an ARDS rat model which showed a dysfunction of blood-gas function and a higher W/D ratio, indicating the occurrence of lung edema and respiratory dysfunction. During ARDS, the activation of inflammatory cells causes the further secretion of inflammatory cytokines such as TNF- α and IL-2 [19]. The exudation of protein-enriched fluid can increase the amounts of proteins and neutrophils or lymphocytes in BALF, further aggravating lung injury, and may cause respiratory failure or death [20]. This study demonstrated that increased amounts of TNF- α and IL-2, plus significantly elevated neutrophils and lymphocytes in BALF in ARDS, suggests severe lung injury.

miRNA has pluripotent functions and can regulate body growth and development, enhancing environmental adaption. Due to its multiple forms of expression, miRNA can be mediated by various physiological and developmental signals [21]. miR-151 has been reported to participate in the regulation of tumors, and cardiovascular and respiratory diseases [22]. However, its role in ARDS has not been reported. This

study demonstrated that the down-regulation of miR-151 in the ARDS group, and the up-regulation of miR-151 in ARDS significantly improved blood-gas, decreased the W/D ratio and MPO activity, and increased SOD activity and suppressed TNF- α and IL-2. Further mechanistic studies found that miR-151 up-regulation in ARDS can suppress the expression of nuclear factor NF- κ B gene and protein expression. NF- κ B plays crucial roles in mediating the gene transcription of inflammatory factors. During the occurrence and progression of lung injury, NF- κ B can modulate multiple factors related to lung injury including inflammatory cytokines and adhesion molecules. The inflammatory mediator can further modulate pulmonary vascular endothelial cells or alveolar epithelial cells, causing a breakdown of the lung-blood barrier [23]. SOD is an important anti-oxidase in lung tissues for the clearance of free oxygen radicals and plays important roles in body oxidation/anti-oxidation homeostasis. MPO is a neutrophilic lysosome enzyme that can reflect the aggregation of neutrophil cells [24, 25]. This study indicated that the modulation of miR-151 could relieve ARDS by inhibiting the mRNA or protein expression of NF- κ B and regulating the oxidative stress response. This study only describes the functional role and regulatory mechanism in an ARDS animal model, and further studies should be performed to investigate the regulatory targets of miR-151 and to illustrate the related pathogenesis mechanisms of ARDS, thus providing evidence for the analysis of ARDS' occurrence and pathological processes.

Conclusion

miR-151 involves down-regulation in a rat ARDS model. The regulation of miR-151 can improve ARDS related pathological changes by modulating the oxidative stress response, alleviating inflammation, and suppressing NF- κ B expression.

Acknowledgements

This work was supported by the Wenzhou Science and Technology Plan Project (No: Y20170128).

Disclosure of conflict of interest

None.

miR-151 in ARDS

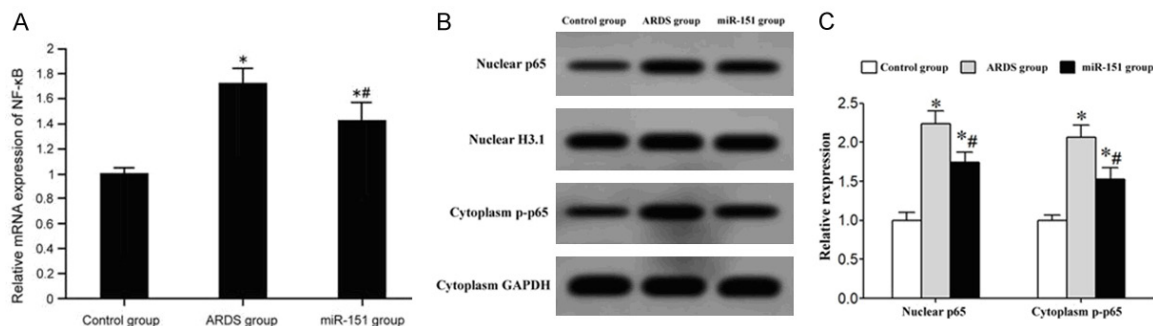


Figure 5. Expression of NF-κB in rat lung tissues. A. NF-κB mRNA expression in rat lung tissues. B. Nuclear p65 and cytoplasmic p-p65 protein expression in rat lung tissues; C. Quantitative analysis of nuclear p65 and cytoplasm p-p65. * $P < 0.05$ compared to the control group; ** $P < 0.05$ compared to the ARDS group.

Address correspondence to: Dr. Zongji Shen, Department of Obstetrics and Gynecology, The First Affiliated Hospital of Soochow University, No. 188, Shizi Road, Suzhou 215006, Jiangsu, China. Tel: +86-0512-65223637; Fax: +86-0512-65223637; E-mail: bhpp953@sina.com

References

- [1] Gronbach J, Ehrhardt H, Zimmer KP, Waitz M. Early pulmonary interstitial emphysema in pre-term neonates-respiratory management and case report in nonventilated very low birth weight twins. *AJP Rep* 2018; 8: e99-e105.
- [2] Meng L, Lv Z, Yu ZZ, Xu D, Yan X. Protective effect of quercetin on acute lung injury in rats with sepsis and its influence on ICAM-1 and MIP-2 expression. *Genet Mol Res* 2016; 15.
- [3] Jabaudon M, Blondonnet R, Constantin JM. Distinct biological effects of time-controlled adaptive ventilation in pulmonary and extrapulmonary acute respiratory distress syndrome: "one small step for rats, one giant leap for humans?" *Crit Care Med* 2018; 46: 1038-1040.
- [4] Morales-Ortiz J, Rondina MT, Brown SM, Grissom C, Washington AV. High levels of soluble triggering receptor expressed on myeloid cells-like transcript (TLT)-1 are associated with acute respiratory distress syndrome. *Clin Appl Thromb Hemost* 2018; 24: 1122-1127.
- [5] Wongsurakiat P, Yuangtrakul N. Performance and applications of bedside visual inspection of airway pressure-time curve profiles for estimating stress index in patients with acute respiratory distress syndrome. *J Clin Monit Comput* 2019; 33: 281-290.
- [6] Nacoti M, Colombo J, Fochi O, Bonacina D, Fazzi F, Bellani G, Bonanomi E. Sevoflurane improves respiratory mechanics and gas exchange in a case series of infants with severe bronchiolitis-induced acute respiratory distress syndrome. *Clin Case Rep* 2018; 6: 920-925.
- [7] Andresen M, Araos J, Wong KY, Leung YC, So LY, Wong WT, Cabrera S, Silva C, Alegria L, Bruhn A, Soto D. Evaluation of meropenem pharmacokinetics in an experimental acute respiratory distress syndrome (ARDS) model during extracorporeal membrane oxygenation (ECMO) by using a PenP beta-lactamase biosensor. *Sensors (Basel)* 2018; 18.
- [8] Diaz JV, Ortiz JR, Lister P, Shindo N, Adhikari NKJ; WHO Critical Care Training Short Course collaborators. Development of a short course on management of critically ill patients with acute respiratory infection and impact on clinician knowledge in resource-limited intensive care units. *Influenza Other Respir Viruses* 2018; [Epub ahead of print].
- [9] Miyoshi H, Inata Y, Takeuchi M. Distinguishing the effects of inhaled nitric oxide and lung recruitment in pediatric acute respiratory distress syndrome: scope for further improvement. *Pediatr Crit Care Med* 2018; 19: 505.
- [10] Wu D, Zeng Y, Fan Y, Wu J, Mulatbieke T, Ni J, Yu G, Wan R, Wang X, Hu G. Reverse-migrated neutrophils regulated by JAM-C are involved in acute pancreatitis-associated lung injury. *Sci Rep* 2016; 6: 20545.
- [11] Desai VG, C Kwekel J, Vijay V, Moland CL, Herman EH, Lee T, Han T, Lewis SM, Davis KJ, Muskhelishvili L, Kerr S, Fuscoe JC. Early biomarkers of doxorubicin-induced heart injury in a mouse model. *Toxicol Appl Pharmacol* 2014; 281: 221-229.
- [12] Katoh M. Cardio-miRNAs and onco-miRNAs: circulating miRNA-based diagnostics for non-cancerous and cancerous diseases. *Front Cell Dev Biol* 2014; 2: 61.
- [13] Isserlin R, Merico D, Wang D, Vuckovic D, Bousette N, Gramolini AO, Bader GD, Emili A. Systems analysis reveals down-regulation of a network of pro-survival miRNAs drives the

- apoptotic response in dilated cardiomyopathy. *Mol Biosyst* 2015; 11: 239-251.
- [14] Yang F, Wei K, Qin Z, Liu W, Shao C, Wang C, Ma L, Xie M, Shu Y, Shen H. MiR-598 suppresses invasion and migration by negative regulation of derlin-1 and epithelial-mesenchymal transition in non-small cell lung cancer. *Cell Physiol Biochem* 2018; 47: 245-256.
- [15] Zheng Y, Liu SQ, Sun Q, Xie JF, Xu JY, Li Q, Pan C, Liu L, Huang YZ. Plasma microRNAs levels are different between pulmonary and extrapulmonary ARDS patients: a clinical observational study. *Ann Intensive Care* 2018; 8: 23.
- [16] Wang S, Li Z, Chen Q, Wang L, Zheng J, Lin Z, Li W. NF-kappaB-induced microRNA-211 inhibits interleukin-10 in macrophages of rats with lipopolysaccharide-induced acute respiratory distress syndrome. *Cell Physiol Biochem* 2018; 45: 332-342.
- [17] Barut F, Ozacmak VH, Turan I, Sayan-Ozacmak H, Aktunc E. Reduction of acute lung injury by administration of spironolactone after intestinal ischemia and reperfusion in rats. *Clin Invest Med* 2016; 39: E15-24.
- [18] Ma S, Lin Y, Deng B, Zheng Y, Hao C, He R, Ding F. Endothelial bioreactor system ameliorates multiple organ dysfunction in septic rats. *Intensive Care Med Exp* 2016; 4: 23.
- [19] Li G, Jia J, Ji K, Gong X, Wang R, Zhang X, Wang H, Zang B. The neutrophil elastase inhibitor, sivelestat, attenuates sepsis-related kidney injury in rats. *Int J Mol Med* 2016; 38: 767-775.
- [20] Peng QY, Zou Y, Zhang LN, Ai ML, Liu W, Ai YH. Blocking cyclic adenosine diphosphate ribose-mediated calcium overload attenuates sepsis-induced acute lung injury in rats. *Chin Med J (Engl)* 2016; 129: 1725-1730.
- [21] Guan Y, Jin X, Liu X, Huang Y, Wang M, Li X. Identification of microRNAs in acute respiratory distress syndrome based on microRNA expression profile in rats. *Mol Med Rep* 2017; 16: 3357-3362.
- [22] Wang T, Lv M, Shen S, Zhou S, Wang P, Chen Y, Liu B, Yu L, Hou Y. Cell-free microRNA expression profiles in malignant effusion associated with patient survival in non-small cell lung cancer. *PLoS One* 2012; 7: e43268.
- [23] Li Y, Zeng Z, Cao Y, Liu Y, Ping F, Liang M, Xue Y, Xi C, Zhou M, Jiang W. Angiotensin-converting enzyme 2 prevents lipopolysaccharide-induced rat acute lung injury via suppressing the ERK1/2 and NF-kappaB signaling pathways. *Sci Rep* 2016; 6: 27911.
- [24] Zhu J, Chen X, Wang H, Yan Q. Catalpol protects mice against renal ischemia/reperfusion injury via suppressing PI3K/Akt-eNOS signaling and inflammation. *Int J Clin Exp Med* 2015; 8: 2038-2044.
- [25] Aldemir M, Karaguzel E, Okulu E, Gudeloglu A, Ener K, Ozayar A, Erel O. Evaluation of oxidative stress status and antioxidant capacity in patients with renal cell carcinoma. *Cent European J Urol* 2015; 68: 415-420.